REPORT DOCUMENTATION PAGE

Form Approved OMB NO. 0704-0188

1. REPORT DATE (DD-MM-YYYY)	2. REPORT TYPE	3. DATES COVERED (From - To)
09-05-2012	Final Report	8-Feb-2011 - 7-Dec-2011

4. TITLE AND SUBTITLE

Terahertz Emitter Based on Frequency Mixing in Microchip Solid-State Laser Cavity Phase I

5a. CONTRACT NUMBER

5b. GRANT NUMBER

W911NF-11-C-0066

5c. PROGRAM ELEMENT NUMBER

665502

6. AUTHORS

Alexander Raspopin

5d. PROJECT NUMBER

5e. TASK NUMBER

5f. WORK UNIT NUMBER

7. PERFORMING ORGANIZATION NAMES AND ADDRESSES

L.C. Pegasus Corporation
225 Long Avenue
Building 15
Hillside, NJ   07205 -

8. PERFORMING ORGANIZATION REPORT NUMBER

9. SPONSORING/MONITORING AGENCY NAME(S) AND ADDRESS(ES)

U.S. Army Research Office
P.O. Box 12211
Research Triangle Park, NC 27709-2211

10. SPONSOR/MONITOR'S ACRONYM(S)

ARO

11. SPONSOR/MONITOR'S REPORT NUMBER(S)

59149-EL-SB1.1

12. DISTRIBUTION AVAILIBILITY STATEMENT

Approved for Public Release; Distribution Unlimited

13. SUPPLEMENTARY NOTES

The views, opinions and/or findings contained in this report are those of the author(s) and should not contrued as an official Department of the Army position, policy or decision, unless so designated by other documentation.

14. ABSTRACT

This project is concerned with development of tunable time-coherent THz source of 0.1-10 THz frequency range. During Phase I of this SBIR we have developed a unique design for nonlinear THz wave generation based on Difference Frequency Generation method, which will deliver the maximum possible energy conversion from optical to THz frequency domains. In the further fabrication stage of this project two types of coherent THz source will be developed: a quasi-cw tunable (0.1/0.3THz - 10 THz) narrowband source with frequency line width 100MHz (line

15. SUBJECT TERMS

nonlinear wave-mixing, THz emission

16. SECURITY CLASSIFICATION OF:			17. LIMITATION OF ABSTRACT	15. NUMBER OF PAGES	19a. NAME OF RESPONSIBLE PERSON
a. REPORT	b. ABSTRACT	c. THIS PAGE			Alexander Raspopin
UU	UU	UU	UU		19b. TELEPHONE NUMBER
					973-923-3028

Report Title

Terahertz Emitter Based on Frequency Mixing in Microchip Solid-State Laser Cavity Phase I

ABSTRACT

This project is concerned with development of tunable time-coherent THz source of 0.1-10 THz frequency range. During Phase I of this SBIR we have developed a unique design for nonlinear THz wave generation based on Difference Frequency Generation method, which will deliver the maximum possible energy conversion from optical to THz frequency domains. In the further fabrication stage of this project two types of coherent THz source will be developed: a quasi-cw tunable (0.1/0.3THz - 10 THz) narrowband source with frequency line width 100MHz (line quality factor $\sim 10^4$, repetition rate $\sim$10kHz) based on OPO single mode laser, and a cw broadband tunable source with frequency line width $\sim$0.3THz based on DFB lasers. Developed multi-layer waveguide will provide the maximum possible efficiency of the nonlinear electromagnetic energy conversion from optical to THz domains. We expect to reach an average output power of 1mW required by the solicitation.

The successful completion of this research project will benefit many new commercial markets in the future. Having coherent, tunable and handy THz source will bring scientists an opportunity to fully explore THz band. Particular applications include: spectroscopic miniature sensors of THz spectra of chem/bio-molecules; next generation THz electronics components with aim to future THz networks and computing chips; vision through clothing at the airport for security purposes; non-destructive imaging through teeth, since THz easily penetrates them; biological hyperspectral imaging of human body.

Enter List of papers submitted or published that acknowledge ARO support from the start of the project to the date of this printing. List the papers, including journal references, in the following categories:

(a) Papers published in peer-reviewed journals (N/A for none)

<u>Received</u>   <u>Paper</u>

   TOTAL:

Number of Papers published in peer-reviewed journals:

(b) Papers published in non-peer-reviewed journals (N/A for none)

<u>Received</u>   <u>Paper</u>

   TOTAL:

Number of Papers published in non peer-reviewed journals:

(c) Presentations

Number of Presentations:

Non Peer-Reviewed Conference Proceeding publications (other than abstracts):

<u>Received</u>   <u>Paper</u>

   TOTAL:

Number of Non Peer-Reviewed Conference Proceeding publications (other than abstracts):

Peer-Reviewed Conference Proceeding publications (other than abstracts):

Received   Paper

  TOTAL:

Number of Peer-Reviewed Conference Proceeding publications (other than abstracts):

(d) Manuscripts

Received   Paper

  TOTAL:

Number of Manuscripts:

Books

Received   Paper

  TOTAL:

Patents Submitted

Patents Awarded

Awards

Graduate Students

NAME	PERCENT_SUPPORTED
FTE Equivalent:	
Total Number:	

Names of Post Doctorates

NAME	PERCENT_SUPPORTED
FTE Equivalent:	
Total Number:	

Names of Faculty Supported

NAME	PERCENT_SUPPORTED
FTE Equivalent:	
Total Number:	

Names of Under Graduate students supported

NAME	PERCENT_SUPPORTED

FTE Equivalent:

Total Number:

Student Metrics
This section only applies to graduating undergraduates supported by this agreement in this reporting period

The number of undergraduates funded by this agreement who graduated during this period: ......

The number of undergraduates funded by this agreement who graduated during this period with a degree in science, mathematics, engineering, or technology fields: ......

The number of undergraduates funded by your agreement who graduated during this period and will continue to pursue a graduate or Ph.D. degree in science, mathematics, engineering, or technology fields: ......

Number of graduating undergraduates who achieved a 3.5 GPA to 4.0 (4.0 max scale): ......

Number of graduating undergraduates funded by a DoD funded Center of Excellence grant for Education, Research and Engineering: ......

The number of undergraduates funded by your agreement who graduated during this period and intend to work for the Department of Defense ......

The number of undergraduates funded by your agreement who graduated during this period and will receive scholarships or fellowships for further studies in science, mathematics, engineering or technology fields: ......

Names of Personnel receiving masters degrees

NAME

Total Number:

Names of personnel receiving PHDs

NAME

Total Number:

Names of other research staff

NAME	PERCENT_SUPPORTED

FTE Equivalent:

Total Number:

Sub Contractors (DD882)

Inventions (DD882)

Scientific Progress

Technology Transfer

L.C.Pegasus
225 Long Ave, Hillside, New Jersey 07205
P.I. Contact: Alexander Raspopin
alexanderraspopin@lcpegasus.com
Tel. 973-923-3028

Contract Administration Point-of-Contact
Ou Li, Contract Administrator
L.C. Pegasus, Inc.
225 Long Ave., Hillside, New Jersey 07205
Phone: (973) 923-3028
Fax: (973) 923-3029
ouli@lcpegasus.com
www.lcpegasus.com

Terahertz Emitter Based on Frequency Mixing in Microchip Solid-State Laser Cavity Phase I

Contract No. W911NF-11-C-0066

Final Technical Report

Performance Period 8 February 2011 – 7 August 2011

Submitted September 9, 2011

Table of Content: p.

A. Project Objectives

The goal of this research project is to make a source of coherent THz radiation using Difference Frequency Generation (DFG) technique by Photomixing of two optical beams with close frequencies in a thin film nonlinear layer. In Phase I the main goal is to formulate a design of such a system which would provide efficient energy transfer from optical laser beams into THz wave.

Thin film layer is a part of the multi-layer waveguide that supports THz mode. Design of the multilayer waveguide must provide Phase Matching Condition (PMC) between THz and optical waves. If this condition satisfied, optical waves will efficiently transfer their energy into THz wave.

In this research project we consider the nonlinear medium, where two main waves with frequencies ω_1 and ω_2 are mixed, to possess a second-order nonlinearity. The nonlinear part of material polarization is expressed as $\mathbf{P_i^{NL} = 2d_{ijk}E_jE_k}$, where $\mathbf{d_{ijk}}$ is the second-order optical susceptibility tensor ($\mathbf{i,j,k=x,y,z}$), and $\mathbf{E_j}$ is the electric field. In general, we can have all four possible output frequencies, namely: $\mathbf{2\omega_1}$, $\mathbf{2\omega_2}$, $\mathbf{\omega_1 + \omega_2}$, and $\mathbf{\omega_1 - \omega_2}$ (DFG). At the end of this Phase I project we clarify this possibilities and also formulate a way which will lead to the waveguide design for Double Harmonic (DH) case $\mathbf{\omega_{output}=2\omega_1}$. This will open the way for much wanted efficient UV generation in 200-300nm spectrum region.

Confining two idler optical beams into a nonlinear thin film waveguide will definitely induce the maximum nonlinear polarization in the medium. Having correct multi-layer waveguide design should lead to efficient excitation of the DFG THz mode by this nonlinear polarization. It is also important to note that a planar design of efficient THz source, which we seek in this project, **will have an ideal case for future integration of this source with planar THz sensing platforms and general THz electronics.**

In Phase I of this SBIR project we have addressed the following **technical objectives**:

1. Design a multi-layer waveguide comprising of the optical and THz wave confinement layers
2. Design a grating coupler embedded in the thin film optical layer. Determine what lens configuration provides the optimize focusing of the idler beams.
3. Predict characteristics of the future THz source. Theoretically estimate efficiency of optical-to-THz power conversion.

B. Work Performed

Work performed in Phase I of this project has been mostly focused on theoretical analysis of the proposed optical to THz energy converter. The main goal has been to suggest a configuration which would provide conversion efficiency much better than has been recently reported.[1]

We have analytically and numerically solved the **following tasks**:

1. Formulated the confinement theory for nonlinear transformation and proposed multi-layer waveguide with TEM THz wave, which maximizes the difference frequency generation.

2. Derived analytically dispersion equations for THz and optical modes.
3. Proved that phase-matching condition, which is necessary for efficient energy transfer from optical to THz wave, is satisfied for the proposed multi-layer waveguide.
4. Proved that absorption losses for TEM THz mode are in acceptable range.
5. Designed a grating In-coupler for optical beams with high excitation efficiency.
6. Derived analytically an expression for energy transformation coefficient and found its numerical estimate for the proposed structure.

C. Results Obtained

Difference frequency generation (DFG) presents a clear path in the development of a coherent THz source.[2-9] In this technique two laser beams with close frequencies are mixed in a second-order nonlinear crystal to produce a difference THz frequency. A typical setup widely used for wavelength conversion is shown in Figure 1.[9] It has a pump Nd:YAG laser, two KTP crystals placed inside a resonator (built by two mirrors M1 and M2) for two close optical wavelength generation and a bulk BNA crystal, taken as an example of a nonlinear crystal, for Difference-Frequency Generation. As it is reported in [9], these authors managed to achieve 13.3% efficiency of pump to idler waves conversion. But idler to THz wave conversion has still been a low (~0.0001-0.001%) efficiency process. [2-9]

A problem with low conversion efficiency comes from the weak nonlinear coupling between optical beams and THz wave. As we show in the Figure 1 the only part needed to be improved in the current, state of the art, DFG THz generation method is the way of excitation of a nonlinear layer.
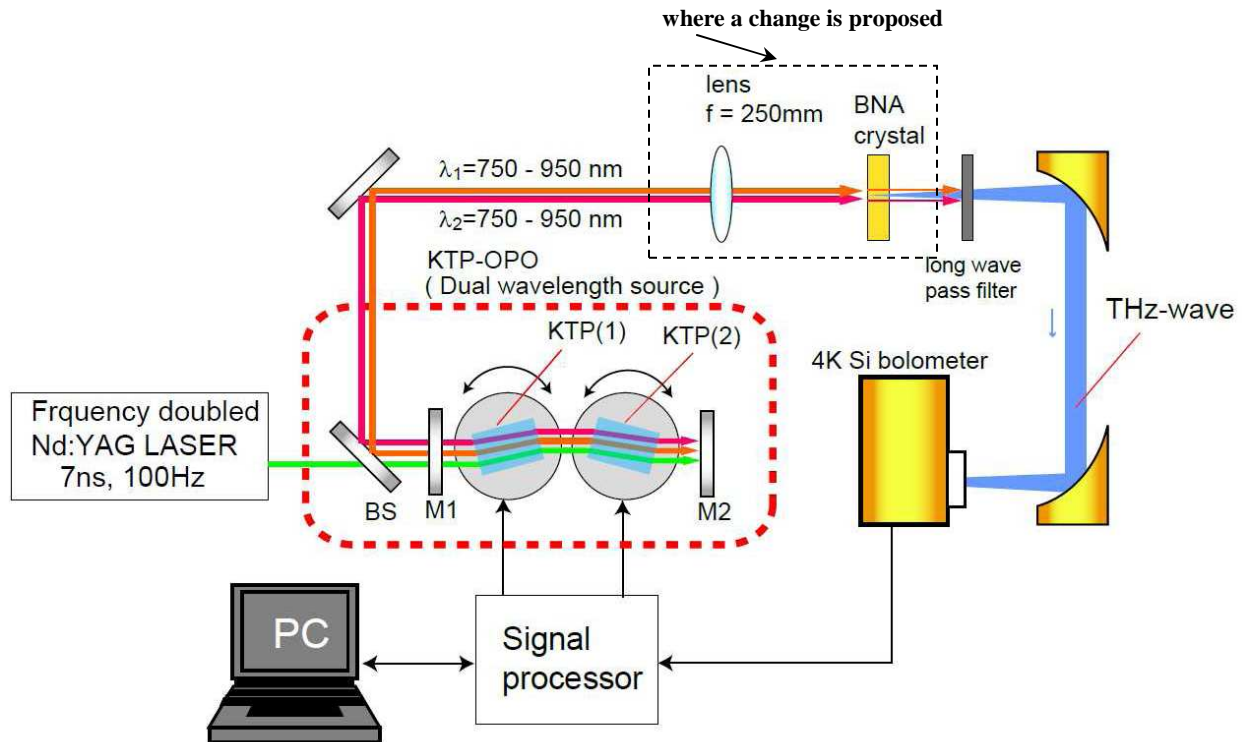

Figure 1. Laser to THz conversion setup based on BNA crystal

To propose an efficient optical-to-THz converter with optimized coupling between e/m waves one needs to formulate an analytical theory of the general energy transformation, which we successfully delivered in this project.

C1. Analytical theory of nonlinear mixing in waveguides

We have derived electromagnetic power of a THz wave and a transformation coefficient in an arbitrary waveguide configuration:

$$P_{THz} = \eta \, P_{\omega_1} P_{\omega_2} \tag{1}$$

$$\eta = \frac{8\pi^2 d_{eff}^2}{n_1 n_2 n_{THz} \, c\varepsilon_0 \lambda_{THz}^2} \frac{1}{A_{eff}} L^2 \operatorname{sinc}^2\left[\frac{\Delta k_z L}{2}\right] \tag{2}$$

$$A_{eff} = \left| \iint \tilde{\vec{E}}_{THz} \cdot \frac{\chi^{(2)}}{|\chi^{(2)}|} : \tilde{\vec{E}}_{\omega_1} \tilde{\vec{E}}_{\omega_2} \, dx \, dy \right|^{-2}, \tag{3}$$

where

$$\iint \tilde{\vec{E}}_\nu \cdot \tilde{\vec{E}}_\mu^* \, dx \, dy = \delta_{\nu\mu}, \tag{4}$$

is the waveguide mode normalization; L is the length of energy conversion along the waveguide; $P_{\omega_1}, P_{\omega_2}$ are the electromagnetic powers of the optical idler modes in the waveguide; $\chi^{(2)}$ is the second-order optical susceptibility tensor, and d_{eff} is its maximum element – nonlinear optical coefficient; n_1, n_2, n_{THz} are the effective propagation indexes of the interacting modes; Δk_z is the wavevector mismatch between the three modes; A_{eff} is the effective area which quantifies the magnitude of the coupling between the nonlinear polarization, excited THz mode and the optical modes.

Possible absorption losses of electromagnetic waves in the waveguide were omitted in Eq.2. Generally they are required to be considered. In this report we lead to a configuration where absorption losses are negligible.

If we suppose that mode configuration of the waveguide is chosen in such way that vector multiplication produces maximum value, what will be achieved by correct choice of the material and orientation-control crystal growth (discussed further in C.5), then the problem of maximizing transformation coefficient splits into two tasks:

1. Maximizing overlap integral $O = \iint \tilde{E}_{THz} \tilde{E}_{\omega_1} \tilde{E}_{\omega_2} \, dx \, dy$ with the normalization condition for interacting modes $\iint \tilde{E}_\nu \cdot \tilde{E}_\mu \, dx \, dy = \delta_{\nu\mu}$,
2. Providing phase matching between modes: $\Delta k_z L \to 0$,
3. Correcting Overlap equation with possible absorption losses of the DFG mode; finding absorption loss for proposed configuration.

<u>**Maximizing the overlap between modes:**</u>

In Figure 2 we show the graphical concept of finding a maximum overlap between optical and THz modes. It is clear that maximum overlap integral achieved in case of fundamental modes.

Electric field of a fundamental mode is of same sign in the whole cross-section of a waveguide. However, low-order optical can also be considered.
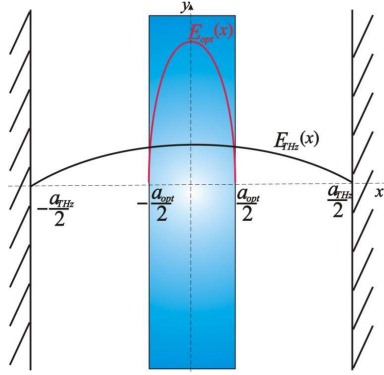

Figure 2. A simple confinement model for overlap between optical and THz modes (under the normalization condition)

For a planar waveguiding structure we obtain the following equation for modes overlap:

$$O(a_{THz}, a_{opt}) = \left(\int_{-\frac{a_{opt}}{2}}^{\frac{a_{opt}}{2}} \sqrt{\frac{2}{a_{THz}}} \cos\left(\frac{\pi x}{a_{THz}}\right) \frac{2}{a_{opt}} \left[\cos\left(\frac{\pi x}{a_{opt}}\right) \right]^2 dx \right)^2 \rightarrow maximum \qquad (5)$$

When deriving Equation 5 we assumed that both idler optical beams only one (same) optical mode in a nonlinear optical layer of the waveguide, which is true because their frequencies are very close.
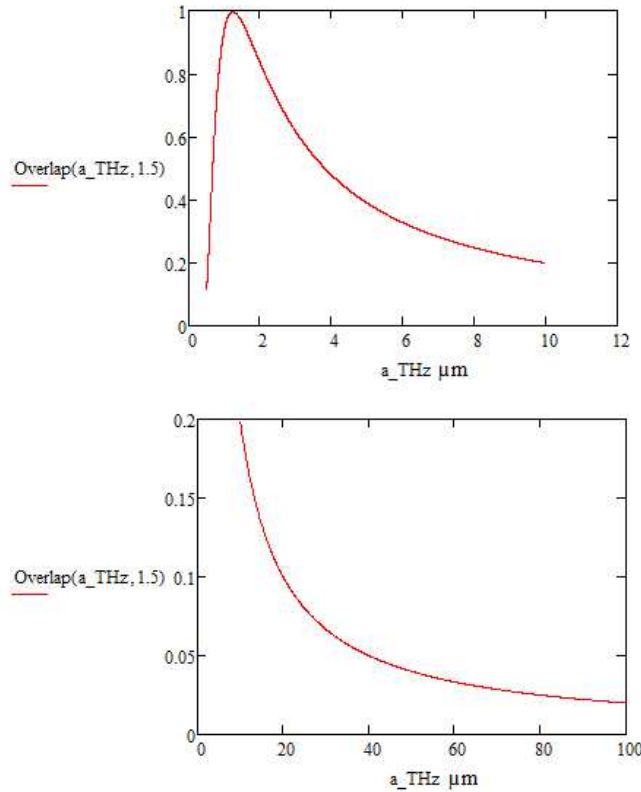

Figure 3. Overlap at a_{opt}=1.5µm (λ_{opt} ~1.5µm) as a function of THz wave thickness

In Figure 3 we show the overlap between modes at 1.5µm optical thickness layer. It drastically decays with the increase of THz wave thickness. Ideally, one has to squeeze THz mode into a size of the optical wavelength to maximize energy conversion between them, which is hard to achieve.

Another interesting and most surprising result we get from mode overlap analysis when we fix the thickness of a THz layer. In Figure 4 we show such case. If , suppose, 100 micron thickness is the thinnest which we are to realize experimentally for terahertz wave then there is no reason to make the optical layer very thin (down to 1 micron), overlap value does not increase much.
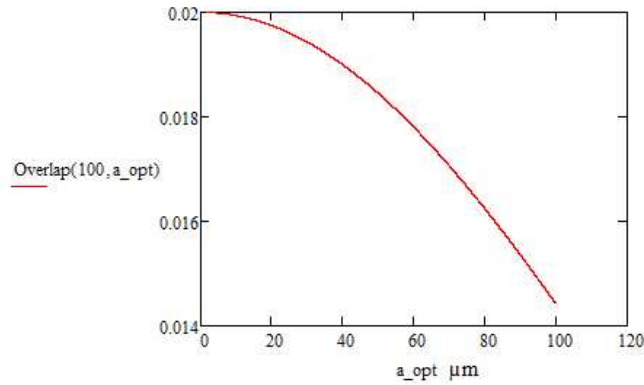

Figure 4. Overlap at a_{THz}=100µm as a function of the optical layer thickness

Following these results we can state that the original idea of using a single metallic plate covered with multi-layer dielectric suggested in Phase I proposal (Figure 5) will not work at THz frequency range (0.1-10THz). The matter is in the confinement of the surface plasmon polaritons mode on smooth metals. The confinement of a THz surface plasmon in perpendicular to metallic surface direction is in order of 10cm, which is very week. Overlap integral of THz wave with optical modes would be very small. This configuration will only work for IR (λ=2-10micron) difference frequency generation.
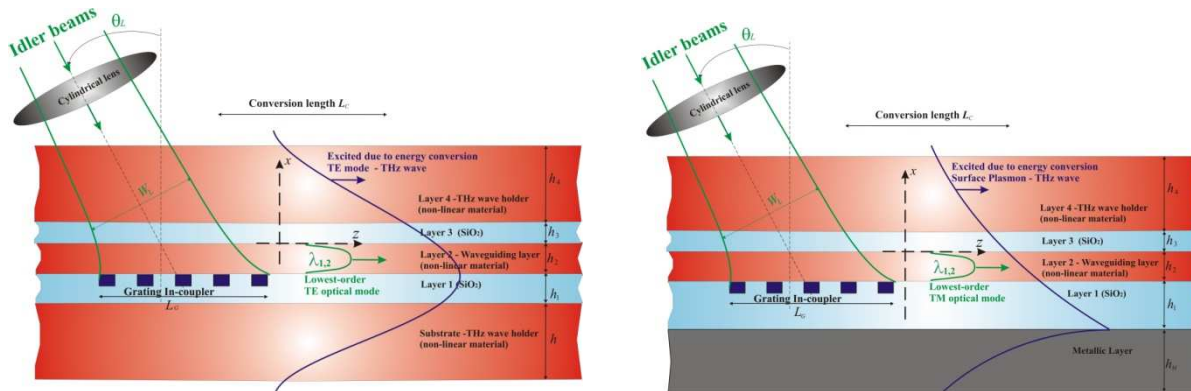

Figure 5. TE and TM configuration for THz generation proposed in Phase I proposal. They will only work for λ=2-10micron difference frequency generation.

Fortunately, we can use a quasi-TEM mode which exists between two parallel metallic plates (Fig.6) at any spacing between them.[10] In the proposed configuration optical beams are confined in a thin film of nonlinear dielectric. There are two concerns: phase-matching between THz and optical modes, and the absorption losses of the TEM THz mode. As it was

experimentally shown in several papers[11,12,13,14] this loss is very low ~ 0.2dB/cm for 100micron spacing between metallic plates. Also a successful confinement of THz wave with frequency ~1THz in a 8micron (!!) thick spacing with negligible absorption losses has been reported.[13]
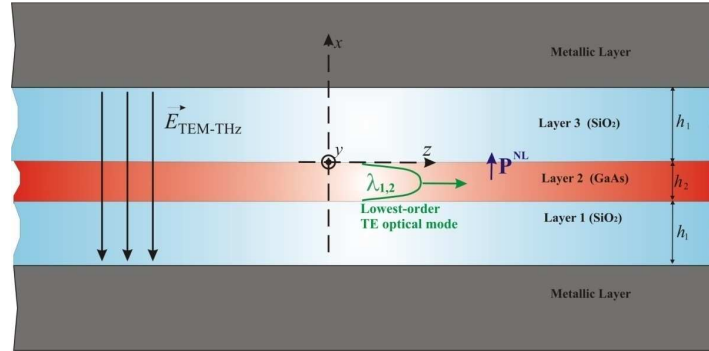

Figure 6. Proposed TEM mode multi-layer waveguide for optical to THz converter.

C2. Dispersion equation for TEM THz mode and satisfaction of the phase-matching condition

It is important to derive a dispersion equation for TEM THz mode and prove that phase-matching between THz and optical modes is possible. Also, this equation will allow finding the exact absorption losses of the THz signal.

In order to find a configuration which would have phase-matching between optical and proposed TEM THz mode we had to solve a dispersion equation for 5-layer planar symmetrical waveguide.

TM guided modes are found in the following form:

$$H_y(x) = \begin{cases} Ae^{-h_3(x-D)}, & x > D, n = n_3 \\ B\cos(h_2x) + \Gamma\sin(h_2x), & d < x < D, n = n_2 \\ \Delta\cosh(h_1x) + E\sinh(h_1x), & -d < x < d, n = n_1 \\ Z\cos(h_2x) + H\sin(h_2x), & -D < x < -d, n = n_2 \\ \theta e^{h_3(x+D)}, & x < -D, n = n_3 \end{cases}, \text{ where } \begin{matrix} h_1^2 = k_z^2 - k_0^2 n_1^2 \\ h_2^2 = -k_z^2 + k_0^2 n_2^2 \\ h_3^2 = k_z^2 - k_0^2 n_3^2 \end{matrix}$$

In case of Quasi-TEM mode located between two metallic plates we need to put:

$$n_1^2 > 0, n_2^2 > 0, Re(n_3^2) < 0$$

We find the dispersion equation for TM Even modes:

$$\frac{h_1}{h_2}\tanh(h_1 d) = -\frac{n_1^2}{n_2^2}\left\{\tan\left[h_2(D-d) + \text{atan}\left(\frac{h_2}{h_3}\frac{n_3^2}{n_2^2}\right)\right]\right\}^{-1} \tag{6}$$

For even modes: $A = \theta, B = Z, \Gamma = -H, E = 0$

$$B = A\left[\cos(h_2D) + \frac{h_3}{h_2}\frac{n_2^2}{n_3^2}\sin(h_2D)\right], B = A\left[\sin(h_2D) - \frac{h_3}{h_2}\frac{n_2^2}{n_3^2}\cos(h_2D)\right]$$

$$\Delta = A\frac{1}{\cosh(h_1d)}\left[\cos(h_2(D-d)) + \frac{h_3}{h_2}\frac{n_2^2}{n_3^2}\sin h_2(D-d)\right]$$

$$\begin{aligned}
1/A^2 = {} & \frac{1}{n_1^2}\left(\frac{1}{\cosh(h_1 d)}\right)^2 \left[\cos\big(h_2(D-d)\big) + \frac{h_3}{h_2}\frac{n_2^2}{n_3^2}\sin\big(h_2(D-d)\big)\right]^2 \left[\frac{\sinh(2h_1 d)}{4h_1} + \frac{d}{2}\right] \\
& + \frac{1}{n_2^2}\left[\frac{D-d}{2}\left(1 + \frac{h_3^2}{h_2^2}\frac{n_2^4}{n_3^4}\right) + \frac{h_3}{2h_2^2}\frac{n_2^2}{n_3^2} + \frac{\sin\big(2h_2(D-d)\big)}{4h_2}\right. \\
& \left. - \frac{h_3}{2h_2^2}\frac{n_2^2}{n_3^2}\cos\big(2h_2(D-d)\big) - \frac{h_3^2}{4h_2^3}\frac{n_2^4}{n_3^4}\sin\big(2h_2(D-d)\big)\right] + \frac{1}{2h_3 n_3^2}
\end{aligned}$$

We have numerically coded Equation 8 for our configuration Al/SiO$_2$/GaAs/SiO$_2$/Al. Parameters for phase matching condition between optical and THz modes are shown in the Proposal.

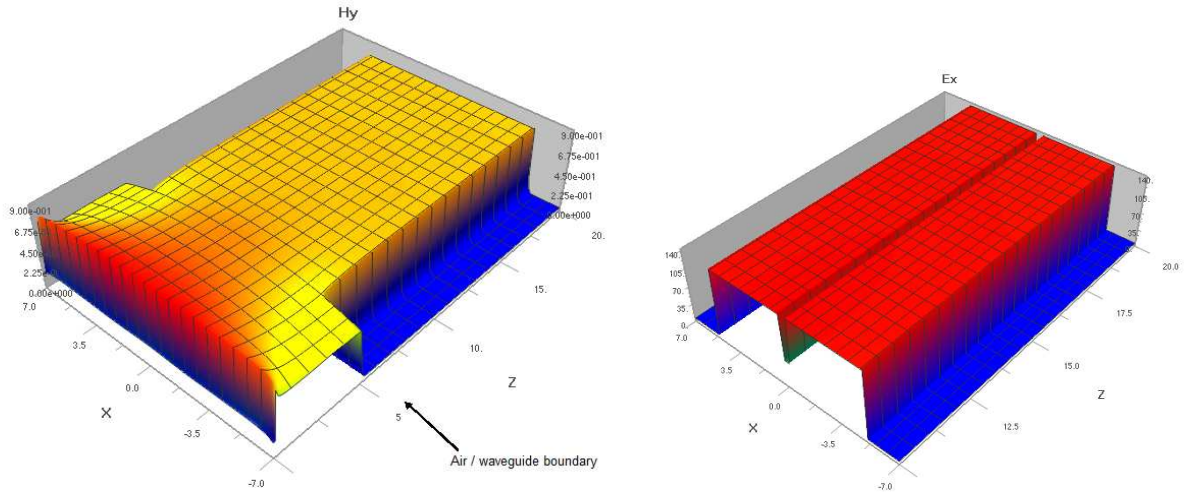We have also obtained TEM modes by FDTD coding (Fig.7,8).

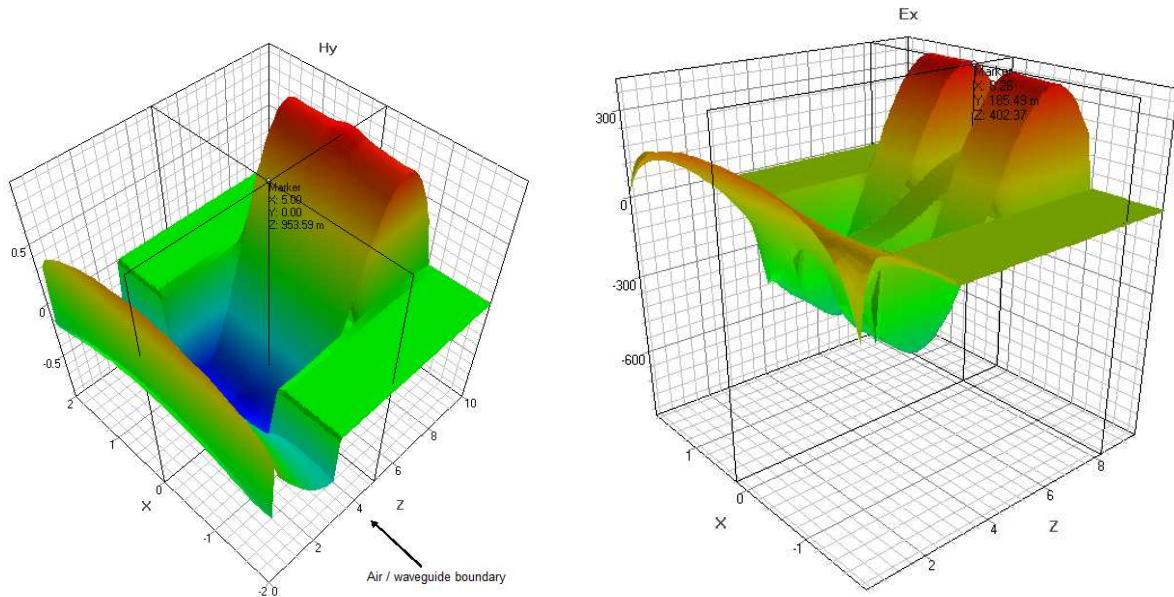Figure 7. Typical picture of TEM mode at λ=300μm, (space dimensions are in microns, amplitude of the fields are shown)

Figure 8. Typical picture of TEM mode at λ=10μm, (space dimensions are in microns, real value of the fields are shown)

C3. Found phase-matched configuration

For difference frequency THz generation PMC can be written as following:

$$\omega_1 n_z(\omega_1) - \omega_2 n_z(\omega_2) = \omega_{\text{THz}} n_z(\omega_{\text{THz}}) \, ,$$

where $\omega_{1,2}$ are the frequencies of the two optical idler beams, $\omega_{\text{THz}} = \omega_1 - \omega_2$ is the difference frequency, $n_z(\omega)$ is the effective refraction index of the propagating mode. In general, the structure of all three modes can differ very much. However, in our case $n_z(\omega_1) \simeq n_z(\omega_2)$ - both idler beams excites the same mode in the waveguide. So, the PMC looks simpler:

$$n_z(\omega_1) = n_z(\omega_{\text{THz}}) \tag{7}$$

As it turns out satisfaction of PMC is feasible for both proposed configuration. Our optical beams are confined in the Layer 2 (Fig.6). After getting a THz TM mode dispersion equation for 5 layer system: metal/dielectric/nonlinear-dielectric/dielectric/metal, optical TE mode dispersion equation for 3 layer system dielectric/nonlinear-dielectric/dielectric and numerically solving them we have obtained the following configuration that exhibit a phase-matching between THz and optical modes:

Al(thickness 10µm)/SiO$_2$(4.8µm)/GaAs(0.385µm)/SiO$_2$(4.8µm)/Al(10µm).

At optical excitation wavelengths $\lambda_1 = 1.5\mu m, \lambda_2 = 1.5 - 1.515\mu m$ there is a full match between effective refractive indexes in this optical and 0.5-3THz range (n$_{\text{eff}}$=2.15). In Figure 9 we have plotted these modes: TEM (λ=300µm), and TE$_1$ (λ=1.5µm).
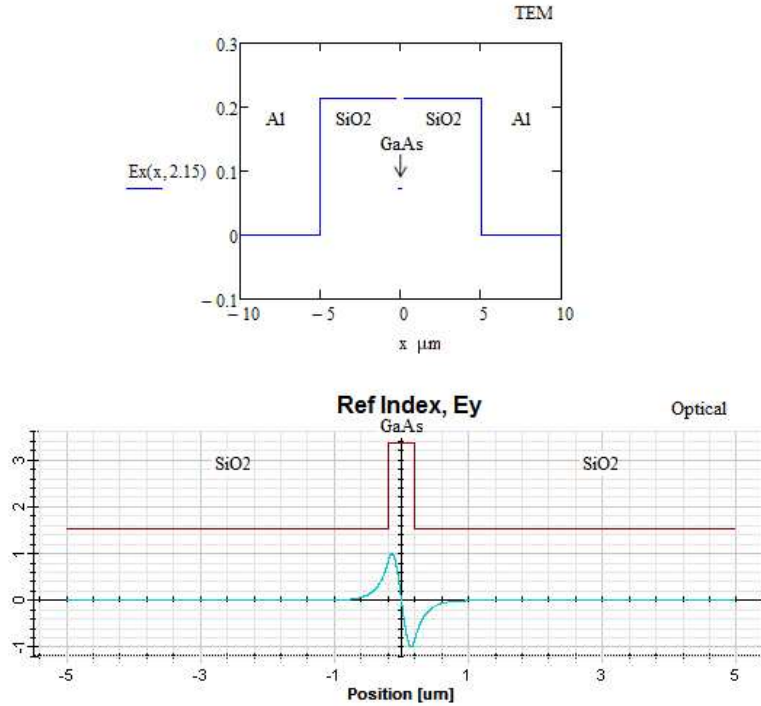

Figure 9. TEM THz mode (λ=300µm), and Optical (λ=1.5µm) mode in the found phase-matched configuration

C4. Absorption losses of the TEM THz wave

To find the absorption losses we seek $\frac{k_z}{k_0} \equiv n_{\text{THz}} = Re(n_{\text{THz}}) + iIm(n_{\text{THz}})$.

For example, let us find the absorption loss for the found phase-matched configuration: Al(thickness 10µm)/SiO$_2$(4.8µm)/GaAs(0.385µm)/SiO$_2$(4.8µm)/Al(10µm). At optical excitation wavelengths $\lambda_1 = 1.5\mu m, \lambda_2 = 1.5 - 1.515\mu m$ there is a full match between effective refractive indexes in this optical and 0.5-3THz range ($Re(n_{\text{THz}}) = n_{optical}^{eff} = 2.146$).

We find the "TEM THz" root of the Dispersion Equation 6 graphically. We have prepared a numerical code for this, and in the Figure 10 we show how the imaginary part of n_{THz} is found. At λ_{THz} =214µm we get $n_{\text{THz}} = 2.146+i0.0073$.
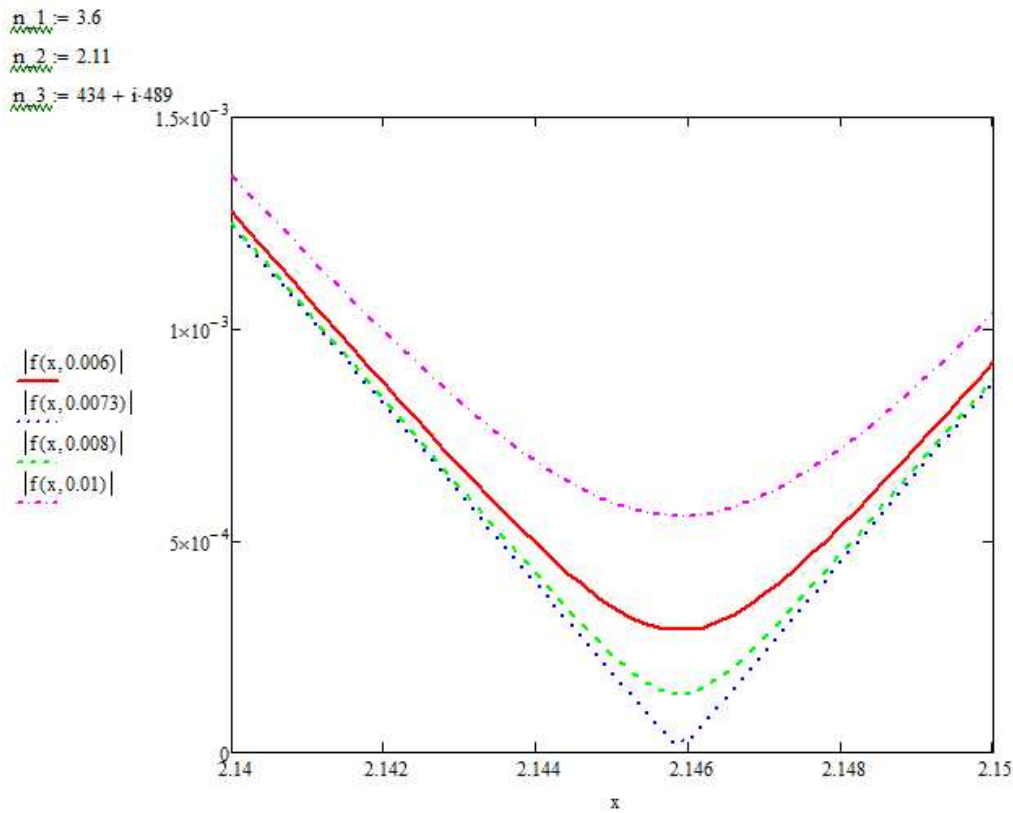

Figure 10. Finding "TEM THz" root graphically λ=214µm. x≡Re(n$_{\text{THz}}$).

Now we can calculate the absorption losses:

$$E_{\text{THz}} = E_{\text{THz}}^0 \exp(-ik_0 n_{\text{THz}} z) \sim \exp(\alpha_{\text{THz}} z), \alpha_{\text{THz}} = k_0 Im(n_{\text{THz}}) \qquad (8)$$

For the considered case (λ=214µm) we get the conversion length $L_c \equiv \alpha_{\text{THz}}^{-1} = 4.7$mm, which is a remarkable huge length for optical effects! Therefore, the proposed coherent energy converter can have up to 1cm waveguide length, which is achievable by CVD and ALD growing methods.

C5. Final design of microstructured multi-layer waveguide and grating In-couplers

Based on the results described above we have formulated two possible design of the proposed optical-to-THz coherent energy converter. As it turns out two configurations are possible: TE optical and TM optical excitations.

TE optical excitation:

As it shown in the Figure 11 the Electric field $\vec{E}_y$ of the TE optical modes excites polarization $\vec{P}_x^{NL}$ of a $\overline{4}3m$ point symmetry group nonlinear semiconductor (GaAs, GaP), which is, in turn, parallel to the electric field of TEM difference frequency wave. Grating coupler will be etched into the SiO_2 layer (Layer 1). Upper metal layer is not "covering" grating grooves, so the laser light can efficiently penetrate SiO_2 layer and excite the grating.
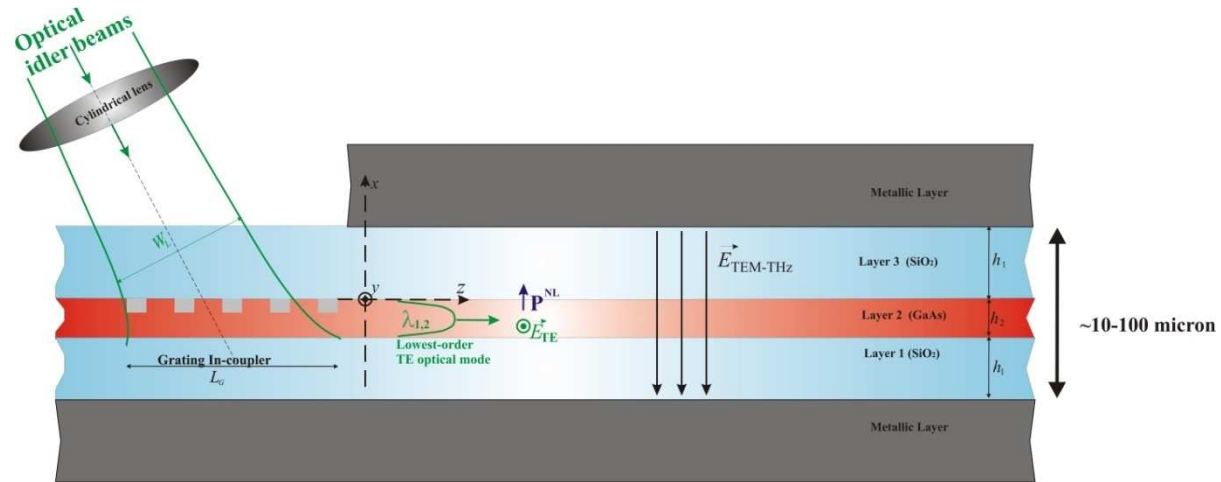

Figure 11. TE optical – TEM THz e/m energy converter based on $\overline{4}3m$ point symmetry group nonlinear material (GaAs, GaP, etc.)

Special requirements have to be met for GaAs layer.[15] It has to be (100) grown layer with a grating grooves parallel to (110) plane of the crystal. In Figure 12 we show crystal orientation for the case of TE optical excitation. Fortunately, there is a developed technique to grow (100) GaAs layer.[16] In Ref.1 ITO coated (200nm thickness) quartz substrates were used for synthesis of thin film GaAs.
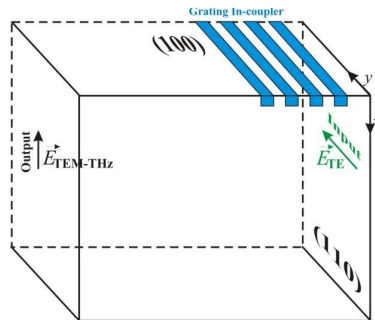

Figure 12. The orientation of $\overline{4}3m$ crystal for converting TE optical input into TEM THz wave. Top surface is (100)

TM optical excitation:

In this case (Fig.13) the dominant electric field in the TM wave, $\vec{E}_x$ ($E_x \gg E_z$) excites the nonlinear polarization $\vec{P}_x^{NL}$ of **3m** symmetry group material (LiNbO$_3$, LiTaO$_3$, etc). LiNbO$_3$ needs to be special c-oriented sputter deposited on SiO$_2$. Fortunately, this technology is already well developed.[17,18,19,20,21]
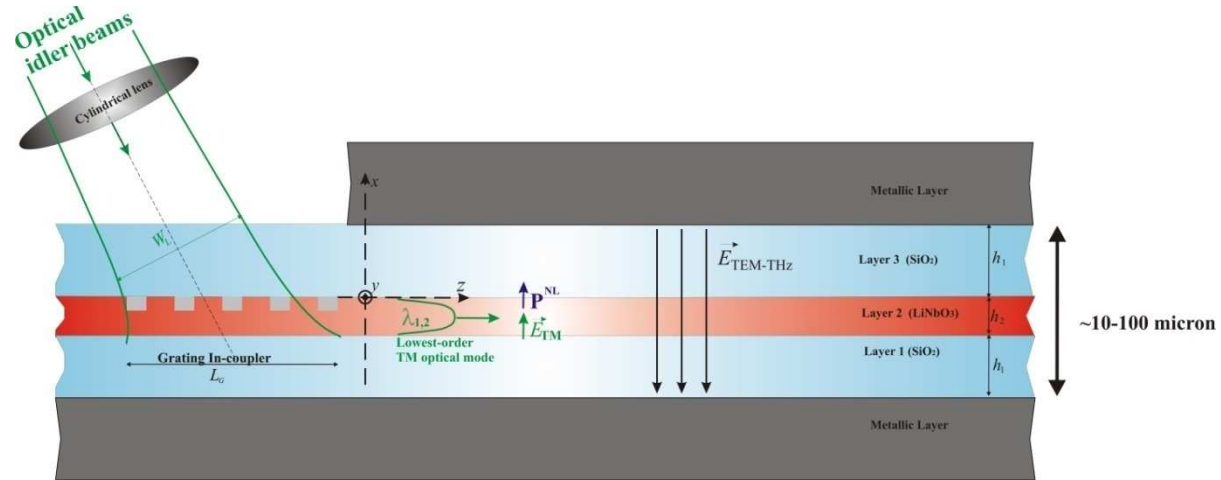

Figure 13. TM optical – TEM THz converter based on 3m symmetry group nonlinear material (LiNbO$_3$, LiTaO$_3$, etc)

Grating In-couper:

Before we estimate the conversion efficiency for the proposed optical-to-THz converter we should provide a design for a grating coupler. Grating coupler serves as an efficient exciter of the optical modes in the thin film nonlinear layer. The PI of this project has already delivered numerically and experimentally such an efficient coupler. The measured efficiency was 80%. By other words, 80% of incident optical power was "inserted" into a thin (325nm thickness) optical waveguide (λ=671nm). [22]

Here we need to prove numerically that we can have this high efficiency couplers for any wavelength, particularly at λ_{opt}=1.5µm, proposed as a pumping wavelength for GaAs nonlinear layer.

In Figure 14 we show a very promising design of such a coupler which works at λ_{opt}=1.5µm, and have coupling efficiency o 60% at the normal (!) incidence. The period of the grating is 700nm, thickness of the GaAs waveguiding layer is 385nm, and groves depth is 120nm. Groves width is 350nm. As of now a 6 µm y-wide beam simulated. However, as PI already proved experimentally,[22] the efficiency stays high even for very y-wide beam (up to several hundred microns).
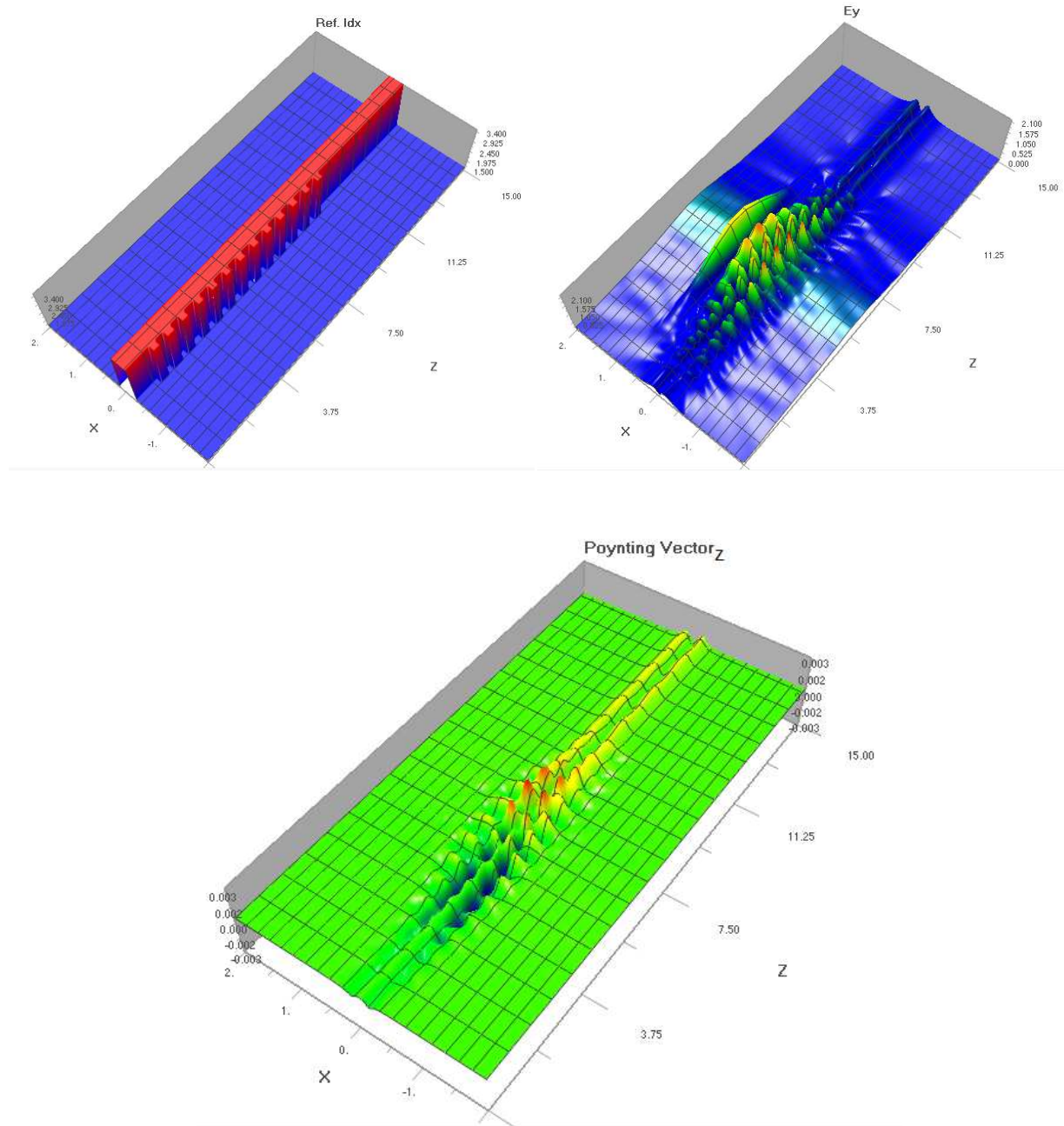
Figure 14. Grating coupler simulated by FDTD numerical method at $\lambda=1.5\mu$m. x,z are in microns. As clearly seen, the optical mode TE_1 is being excited apparently only in +z-direction at normal (!) incidence.

C6. Energy transformation coefficient in general case with absorption losses

We have derived a general equation for energy transformation efficiency. Here we show a brief derivation of this equation.

In undepleted case, when optical powers $P_{1,2}$ do not change much along the propagation (waveguide) direction we have:

$$\frac{dA_{\mathrm{THz}}}{dz} = -\alpha_{\mathrm{THz}}A_{\mathrm{THz}} + kA_1A_2^*e^{-i\Delta k_z z}, \tag{9}$$

where A_{THz} is the amplitude of the THz wave, $A_{1,2}$, are the amplitudes of two optical modes, k is proportional to overlap between modes, $k \sim \left| \iint \vec{\tilde{E}}_{THz} \cdot \frac{\chi^{(2)}}{|\chi^{(2)}|} : \vec{\tilde{E}}_{\omega_1}\vec{\tilde{E}}_{\omega_2} \, dx\, dy \right|^2$, Δk_z is the wave vector mismatch between optical and THz modes, is α_{THz} the absorption loss of the THz mode mainly occurring in the metallic layers (Fig.6).

Solution of the Differential Equation 1 we seek in the following form:

$$A_{\mathrm{THz}}(z) = f(z)e^{-\alpha_{\mathrm{THz}}z},$$

which lead to:

$$\frac{df}{dz} = kA_1A_2^*e^{(\alpha_{\mathrm{THz}}-i\Delta k_z)z} \ .$$

After integrating (9) we obtain the equation for energy transformation coefficient:

$$\eta = \frac{P_{\mathrm{THz}}}{P_1P_2} = \frac{8\pi^2 d_{eff}^2}{n_1 n_2 n_{THz}\, c\varepsilon_0\lambda_{\mathrm{THz}}^2} \frac{1}{A_{eff}} \frac{(1+e^{-2\alpha_{\mathrm{THz}}L}-2e^{-\alpha_{\mathrm{THz}}L}\cos(\Delta k_z L))}{(\alpha_{\mathrm{THz}}^2+\Delta k_z^2)}, \tag{10}$$

where L is the mode interaction length; $A_{eff} = \left| \iint \vec{\tilde{E}}_{THz} \cdot \frac{\chi^{(2)}}{|\chi^{(2)}|} : \vec{\tilde{E}}_{\omega_1}\vec{\tilde{E}}_{\omega_2} \, dx\, dy \right|^{-2}$ is the overlap surface between modes, which obeys the mode normalization condition:

$$\iint \vec{\tilde{E}}_\nu(x,y) \cdot \vec{\tilde{E}}_\mu^{\ *}(x,y) \ dx\, dy = \ \delta_{\nu\mu},$$

n_1, n_2, n_{THz} are the effective propagation indexes of the interacting modes; $\chi^{(2)}$ is the second-order optical susceptibility tensor, and d_{eff} is its maximum element – nonlinear optical coefficient.

Equation 10 is very general equation that describes coherent energy transfer between two optical idler modes and the THz mode in any waveguide geometry. The only assumption of undepleted regime for optical modes can be corrected in our further research.

This equation takes into account both factors which limit the efficiency of the energy transformation: absorption losses and the phase mismatch between the modes. As we have shown in C.3 of this report, we have found a configuration which provides the phase-matching condition: $\Delta k_z L \rightarrow 0$. In this case the only limiting factor is the absorption loss of the THz mode. Equation 10 will transform into the following:

$$\eta = \frac{P_{\mathrm{THz}}}{P_1P_2} = \frac{8\pi^2 d_{eff}^2}{n_1 n_2 n_{THz}\, c\varepsilon_0\lambda_{\mathrm{THz}}^2} \frac{1}{A_{eff}} \frac{1}{(\alpha_{\mathrm{THz}}^2)} \tag{11}$$

Here we assumed that the length of the waveguide will be slightly more than the conversion length, which in the phase-matched case equal to $L_C = \frac{1}{\alpha_{\mathrm{THz}}}$.

Applying Equation 11 to the proposed TEM THz waveguide:

It would be of great help for this project to have an analytical expression for the energy transformation coefficient in terms of parameters of the proposed waveguide design (Fig.6). A unique property of the TEM mode, which is its step-function dependence on the normal coordinate (x-axis, Fig. 6,9), helped us derive such an equation.

By introducing the characteristic optical beams space confinement in y-direction L_y, we have

$$\frac{1}{A_{eff}} = \left| \iint \vec{\tilde{E}}_{THz}(x,y)\vec{\tilde{E}}_{\omega_1}(x,y)\vec{\tilde{E}}_{\omega_2}(x,y)\, dx\, dy \right|^2 \cong L_y^2 \left| \iint \vec{\tilde{E}}_{THz}(x)\vec{\tilde{E}}_{\omega_1}(x)\vec{\tilde{E}}_{\omega_2}(x)\, dx \right|^2 . \qquad (12)$$

Recalling that the optical frequencies are very close: $\omega_1 - \omega_2 = \omega_{THz} \ll \omega_{1,2}$, we have their mode structures the same: $\vec{\tilde{E}}_{\omega_1}(x) = \vec{\tilde{E}}_{\omega_2}(x)$.

Optical modes are confined in a thin nonlinear layer, where TEM THz electric field is constant. So, we get:

$$\frac{1}{A_{eff}} \cong L_y^2 \left(\vec{\tilde{E}}_{THz}(x = x_{GaAs}) \right)^2 \iint \left| \vec{\tilde{E}}_{\omega_1}(x) \right|^2 dx.$$

After applying the normalization condition TEM THz mode we obtain:

$$\frac{1}{A_{eff}} \cong \left(\vec{\tilde{E}}_{THz}(x = x_{GaAs}) \right)^2 ,$$

and using D field boundary condition:

$$D_{x,\,GaAs}^{THz} = D_{x,\,SiO2}^{THz}$$

we finally obtain:

$$\frac{1}{A_{eff}} \cong \frac{1}{L_y h_{GaAs}\left[1 + \left(\frac{n_{GaAs}^{THz}}{n_{SiO2}^{THz}} \right)^4 \left(\frac{h_{SiO2}}{h_{GaAs}} \right) \right]}.$$

Energy conversion efficiency will be found as

$$\eta = \frac{P_{THz}}{P_1 P_2} \cong \frac{8\pi^2 d_{eff}^2}{n_1 n_2 n_{THz}\, c\varepsilon_0 \lambda_{THz}^2} \left(\frac{1}{L_y h_{GaAs}\left[1 + \left(\frac{n_{GaAs}^{THz}}{n_{SiO2}^{THz}} \right)^4 \left(\frac{h_{SiO2}}{h_{GaAs}} \right) \right]} \right) \frac{1}{(\alpha_{THz}^2)} . \qquad (13)$$

Now we can easily predict the conversion efficiency coefficient for our multi-layer waveguide once we know the exact absorption losses.

Estimate of energy conversion efficiency:

We can finally calculate the expected energy conversion efficiency. We will assume that grating coupler provides maximum ~100% excitation efficiency. Eq. 13 transforms into following:

$$\eta = \frac{P_{\text{THz}}}{P_1 P_2} \cong \frac{2 d_{eff}^2}{n_1 n_2 n_{THz}\, c\varepsilon_0} \left(\frac{1}{L_y h_{\text{GaAs}}\left[1 + \left(\frac{n_{\text{GaAs}}^{\text{THz}}}{n_{\text{SiO2}}^{\text{THz}}}\right)^4 \left(\frac{h_{\text{SiO2}}}{h_{\text{GaAs}}}\right)\right]} \right) \frac{1}{(Im(n_{THz})^2)} \cdot \tag{14}$$

It is interesting that Eq.14 does not depend explicitly on optical idler beam wavelengths, neither on generated THz wavelength. So, we obtain:

For LiNbO3 at $\lambda_{1,2}=1.5\mu m$

$$\eta = \frac{2\cdot\left(175\cdot 10^{-12}\right)^2}{3\cdot 10^8\cdot 8.85\cdot 10^{-12}\cdot 2\cdot 2\cdot 2\cdot 0.005^2\cdot 100\cdot 10^{-6}\cdot 0.385\cdot 10^{-6}\left[1 + \left(\frac{5.2}{2.11}\right)^4\cdot\frac{\left(10\cdot 10^{-6} - 0.385\cdot 10^{-6}\right)}{\left(0.385\cdot 10^{-6}\right)}\right]} = 3.249\times 10^{-6}$$

For GaAs at $\lambda_{1,2}=1.5\mu m$

$$\eta = \frac{2\cdot\left(50\cdot 10^{-12}\right)^2}{3\cdot 10^8\cdot 8.85\cdot 10^{-12}\cdot 2\cdot 2\cdot 2\cdot 0.005^2\cdot 100\cdot 10^{-6}\cdot 0.385\cdot 10^{-6}\left[1 + \left(\frac{3.6}{2.11}\right)^4\cdot\frac{\left(10\cdot 10^{-6} - 0.385\cdot 10^{-6}\right)}{\left(0.385\cdot 10^{-6}\right)}\right]} = 1.15\times 10^{-6}$$

Obtained conversion efficiency numbers are not optimized. We think that by squeezing optical beam in y-direction down to 30 micron and additional squeeze of TEM mode down to 1-2 microns in x-direction can improve efficiency up to 10^{-4} value.

Also, there are organic DAST and BNA crystals which have $d_{eff} \sim 10^3$ pm/V.[23,24,25] If they could be employed in our micron thick waveguide geometry – they would increase η up to 10^{-2} value. The best value of conversion efficiency recently reported in Ref. [1] is $1.3\cdot 10^{-7}$ W^{-1}.

D. Estimate of Technical Feasibility

In this Phase I SBIR project we have performed a vigorous theoretical analysis of the proposed multi-layer waveguide. To our best knowledge no one yet in the scientific world has done any similar analysis. This research effort outlines and finds the best design configuration for Difference Frequency Generation (DFG).

The objective of this particular project has been to formulate a design for THz DFG. But the approach which we have developed within this project is not limited to DFG and neither to THz frequency range as a goal. This approach will be the best for deep UV, IR (LWIR, MWIR, SWIR) radiation generation. It will lead to some unique waveguiding designs for these e/m wave ranges. The designs will be different from the one for THz presented here, but they will be also the most efficient.

In this report we have not specified any sources of the idler optical beams. The choice of them is arbitrary. It is clear that the best performance will be with coherent laser beams, since they can be squeezed easily.

Another important aspect is the coherence of the THz signal generated in the proposed converter. Time coherence of the THz signal will be transferred (translated) from idler optical signal without any change. There is no electronic transition between bands involved in this nonlinear conversion technique as contrary to "photoconductive antenna" method[26] where electron scattering limits coherence of the DFG signal. In our scheme the narrower the optical lasing wavelength, the narrower the generated THz line.

We have already mentioned that the success of this project now lies in advanced area of the microfabrication. We have specified the references where thin $LiNbO_3$ or GaAs layers were successfully grown and tested on their values of nonlinear coefficient.

This project is concerned with development of tunable time-coherent THz source of 0.1-10 THz frequency range. In the further fabrication stage of this research two types of coherent THz source will be developed: a quasi-cw tunable narrowband source with frequency line width 100MHz (line quality factor ~10^4, repetition rate ~10kHz), and a cw broadband tunable source with frequency line width ~0.3THz. These two lasers will be based on different pump lasers: OPO with a solid state single mode laser and with two DFB lasers, which are frequency tuned by temperature. Tunability range of will be 0.1/0.3THz - 10 THz. Our unique multi-layer waveguide will provide us the maximum possible efficiency of the nonlinear electromagnetic energy conversion from optical to THz frequency domains. We expect to reach an average output power of 1mW required by the solicitation.

The successful completion of this project in the future will benefit many new commercial markets. Having coherent, tunable and handy THz source will bring scientists an opportunity to fully explore THz band. Particular applications include: spectroscopic miniature sensors of THz spectra of chem/bio-moleculas; next generation THz electronics components with aim to future THz networks and computing chips; vision through clothing at the airport for security purposes; non-destructive imaging through teeth, since THz easily penetrates them; biological hyperspectral imaging of human body.

References:

1. Chad Staus, Thomas Kuech, and Leon McCaughan, "Continuously phase-matched terahertz difference frequency generation in an embeddedwaveguide structure supporting only fundamental mode" Optics Express **16**, 13296 (2008).

2. K. Kawase, J. Shikata, and H. Ito: "Terahertz wave parametric source", Journal of Physics D: Applied Physics **35**, R1 (2002).

3. T. Tanabe, K. Suto, J. Nishizawa, K. Saito, and T. Kimura, "Tunable terahertz wave generation in the 3- to 7-THz region from GaP" Applied Physics Letters **83**, 237 (2003).

4. Wei Shi, Yujie J. Ding, Nils Fernelius, and Konstantin Vodopyanov, "Efficient, tunable, and coherent 0.18 5.27-THz source based on GaSe crystal: erratum" Optics Letters **28**, 136 (2003).

5. K. Kawase, T. Hatanaka, H. Takahashi, K. Nakamura, T. Taniuchi, and H. Ito, "Tunable terahertz-wave generation from DAST crystal by dual signal-wave parametric oscillation of periodically poled lithium niobate" Optics Letters, **25**, 1714-1716 (2000).

6. A. Rice, Y. Jin, X. F. Ma, X. C. Zhang, D. Bliss, J. Larkin, and M. Alexander, "Terahertz optical rectification from <110> zinc blende crystals" Applied Physics Letterrs **64**, 1324 (1994).

7. Takayuki Shibuya, Takuya Akiba, Koji Suizu, Hirohisa Uchida, Chiko Otani, and Kodo Kawase, "Terahertz-Wave Generation Using a 4-Dimethylamino-N-methyl-4-stilbazolium tosylate Crystal Under Intra-Cavity Conditions", Applied Physics Express **1**, 042002 (2008).

8. Y. Takahashi, S. Onduka, S. Brahadeeswaran, M. Yoshimura, Y. Mori, T. Sasaki, "Development of DAST crystals with high damage tolerance" Optical Materials **30**, 116 (2007).

9. Katsuhiko Miyamoto, Seigo Ohno, Masazumi Fujiwara, Hiroaki Minamide, Hideki Hashimoto, and Hiromasa Ito, "Optimized terahertz-wave generation using BNA-DFG" Optics Express **17**, 14832 (2009).

10. N. Marcuvitz, Waveguide Handbook (Peregrinus, London, 1993), Chap. 2, p. 64.

11. H. Cao, R. A. Linke, A. Nahata, "Broadband generation of terahertz radiation in a waveguide" Optics Letters 29, 1751 (2004)

12. R. Mendis and D. M. Mittleman, "An investigation of the lowest-order transverse-electric TE1 mode of the parallel-plate waveguide for THz pulse propagation"J. Opt. Soc. Am. B Vol. 26, A6 (2009)

13. Michael Theuer, Rene Beigang, and Daniel R. Grischkowsky, "Adiabatic compression of terahertz waves using metal flares" APPLIED PHYSICS LETTERS 96, 191110 (2010)

14. Yun-Shik Lee, Principles of Terahertz Science and Technology, *Springer Science+Business Media, LLC*, page 184. (2009)

15. A. Yariv "Coupled-Mode Theory for Guided-Wave Optics" IEEE Journal of Quantum Electronics, Vol. QE-9, NO 9, 919 (1973)

16. M. Chamekh, M. Lajnef, L. Zerroual, and R. Chtourou, "Synthesis and characterization of GaAs thin films grown on ITO substrates" Eur. Phys. J. Appl. Phys. 52, 20502 (2010)

17. Charles H. J. Huang and Thomas A. Rabson, "Low-loss thin-film LiNbO3 optical waveguide sputtered onto a SiO2/Si substrate", OPTICS LETTERS 18, 811 (1993)

18. S. Tan, T. Gilbert, C.-Y. Hung, T. E. Schlesinger, and M. Migliuolo, "Sputter deposited c-oriented LiNbO3 thin films on SiO2", J. Appl. Phys. 79, 3548 (1996)

19. S. Y. Lee and R. S. Feigelson,"c-axis lithium niobate thin film growth on silicon using solid-source metalorganic chemical vapor deposition" J. Mater. Res., Vol. 14, 2662 (1999)

20. G. Balestrino et al, "Epitaxial LiNbO3 thin films grown by pulsed laser deposition for optical waveguides", APPLIED PHYSICS LETTERS 78, 1204 (2001)

21. Monika Tomar, Vinay Gupta, Abhai Mansingh and K Sreenivas "Temperature stability of c-axis oriented LiNbO3/SiO2/Si thin film layered structures" J. Phys. D: Appl. Phys. 34 2267 (2001)

22. Gillman, E., Raspopin, A., et al. "Polymer-assisted conformal coating of TiO2 thin films", Journal of Applied Physics 108, 044310 (2010)

23. Takayuki Shibuya, Takuya Akiba, Koji Suizu, Hirohisa Uchida, Chiko Otani, and Kodo Kawase, "Terahertz-Wave Generation Using a 4-Dimethylamino-N-methyl-4-stilbazolium tosylate Crystal Under Intra-Cavity Conditions", Applied Physics Express **1**, 042002 (2008).

24. Y. Takahashi, S. Onduka, S. Brahadeeswaran, M. Yoshimura, Y. Mori, T. Sasaki, "Development of DAST crystals with high damage tolerance" Optical Materials **30**, 116 (2007).

25. Katsuhiko Miyamoto, Seigo Ohno, Masazumi Fujiwara, Hiroaki Minamide, Hideki Hashimoto, and Hiromasa Ito, "Optimized terahertz-wave generation using BNA-DFG" Optics Express **17**, 14832 (2009).

26. http://www.dmphotonics.com/Photoconductive_Antenna_THz.htm